Available online at www.sciencedirect.com
SCIENCE DIRECT®
Journal of Sound and Vibration 273 (2004) 457–475
JOURNAL OF SOUND AND VIBRATION
www.elsevier.com/locate/jsvi

Free vibration analysis of a cracked beam by finite element method

D.Y. Zheng*, N.J. Kessissoglou

School of Engineering, James Cook University, Townsville, QLD 4811, Australia

Received 26 November 2002; accepted 28 April 2003

Abstract

In this paper, the natural frequencies and mode shapes of a cracked beam are obtained using the finite element method. An 'overall additional flexibility matrix', instead of the 'local additional flexibility matrix', is added to the flexibility matrix of the corresponding intact beam element to obtain the total flexibility matrix, and therefore the stiffness matrix. Compared with analytical results, the new stiffness matrix obtained using the overall additional flexibility matrix can give more accurate natural frequencies than those resulted from using the local additional flexibility matrix. All the elements in the overall additional flexibility matrix are computed by 128-point (1D) or (128×128)-point (2D) Gauss quadrature, and then further best fitted using the least-squares method. The explicit form best-fitted formulas agree very well with the numerical integration results, and are very convenient for use and valuable for further reference. In addition, the authors constructed a shape function that can perfectly satisfy the local flexibility conditions at the crack locations, which can give more accurate vibration modes.

1. Introduction

The cracked beam problem has attracted the attention of many researchers in recent years. Various kinds of analytical, semi-analytical and numerical methods have been employed to solve the problem of a cracked beam [1–12]. A common method is to use the finite element method (FEM). The key problem in using FEM is how to appropriately obtain the stiffness matrix for the cracked beam element. The most convenient method is to obtain the total flexibility matrix of the element first and then take inverse of it. The total flexibility matrix of the cracked beam element includes two parts. The first part is the original flexibility matrix of the intact beam. The second

*Corresponding author.
E-mail addresses: dingyang.zheng@jcu.edu.au (D.Y. Zheng), nicole.kessissoglou@jcu.edu.au (N.J. Kessissoglou).

0022-460X/03/$ - see front matter © 2003 Elsevier Ltd. All rights reserved.
doi:10.1016/S0022-460X(03)00504-2

part is the additional flexibility matrix due to the existence of the crack, which leads to energy release and additional deformation of the structure. Papadopoulos and Dimarogonas [1] elegantly presented the 'local flexibility matrix' of a beam due to the existence of the crack by the integration of stress intensity factors. Their obtained flexibility matrix is indeed a 'local' one, as we can see in their paper that $K_{I2} = K_{I3} = 0$, where P_2 and P_3 are the shearing forces. The local flexibility matrix is especially appropriate for the analysis of a cracked beam if one employs an analytical method by solving the differential equations piecewisely [2]. It is also appropriate to use a semi-analytical method by using the modified Fourier series [3–5], mechanical impedance method [6], Rayleigh–Ritz method [7], or transfer matrix method [8]. When FEM is used, to obtain the stiffness matrix it is necessary to take into account the effect of the distance between the right hand side end node of the element and the crack location, i.e., L_c (see Figs. 1 and 2). The reason is that the shearing force P_2 also contributes to the opening type (i.e., K_{I2}) of the crack through the bending moment $P_2 L_c$. This problem has been previously ignored in Refs. [9,10], in which the local flexibility matrix is directly added to the flexibility matrix of the corresponding uncracked element to obtain the total flexibility matrix. This is not very accurate because the former matrix is to describe the local behaviour in the vicinity of the crack region, while the later matrix describes the overall behaviour of the beam element. In this paper, the authors derived new FEM formulas to overcome the existing shortcomings by adding an 'overall additional flexibility matrix', which describes the overall behaviour of flexibility due to the presence of the crack, onto the flexibility matrix of the corresponding intact beam. By comparing the FEM results obtained in this paper with available existing analytical methods, the new stiffness matrix can indeed give more accurate results than those obtained from using the local flexibility matrix. Moreover, all the elements of the overall additional flexibility matrix are computed by 128-point (1D) or 128×128 (2D) Gauss quadrature and then further best fitted using the least-squares method. The best-fitted formulas agree very well with the numerical integration results. They are convenient for use and valuable for further reference.

Once the stiffness matrix of a cracked beam element is successfully obtained by 'going detour' (i.e., obtaining the total flexibility matrix first and then taking inverse of it), standard FEM procedure can be followed, which will lead to a generalized eigenvalue problem and thus the

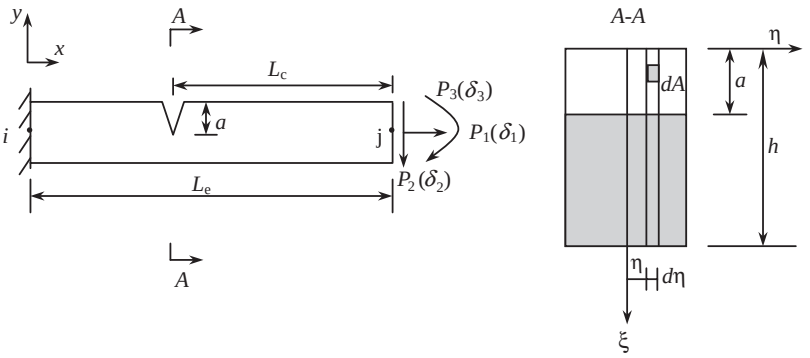

Fig. 1. A typical cracked beam element subjected to axial force, shearing force and bending moment (rectangular cross-sectional beam).

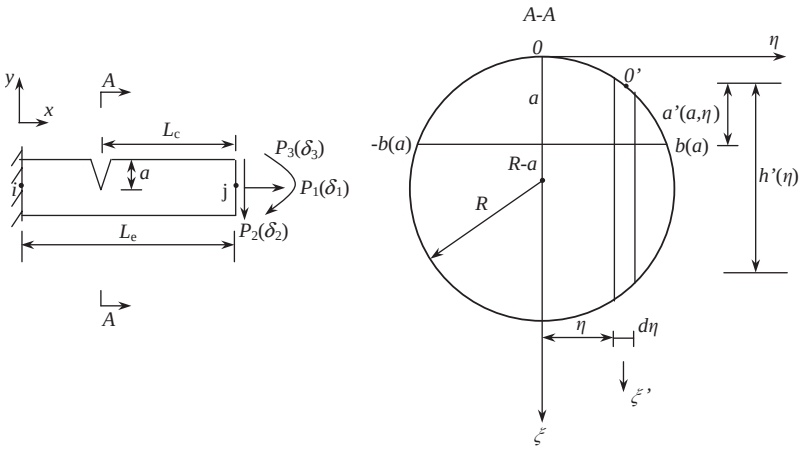

Fig. 2. A typical cracked beam element subjected to axial force, shearing force and bending moment (circular cross-sectional beam).

natural frequencies can be obtained. However, it is worth noting that it is not appropriate to compute the vibration modes for the elements having cracks by still using the standard Hermitian interpolation as in the common FEM method. This problem is seemly ignored by many researchers when using the 'detour method'. In this paper, the relationship between the displacements at the crack locations and those at the two end nodes of a cracked beam element is derived (see Eq. (65)). The presented shape function in this paper can perfectly satisfy the local flexibility conditions as well as continuity conditions at the crack locations, which can give more accurate vibration modes.

2. Stiffness matrix K_c of a cracked beam element

2.1. Elements of the overall additional flexibility matrix $\boldsymbol{C}_{ovl}$

Figs. 1 and 2 show a typical cracked beam element with a rectangular and a circular cross-section, respectively. The left hand side end node i is assumed fixed, while the right hand side end node j is subjected to axial force P_1, shearing force P_2 and bending moment P_3. The corresponding generalized displacements are denoted as δ_1, δ_2 and δ_3. In Figs. 1 and 2, a denotes the crack depth and L_c denotes the distance between the right hand side end node j and the crack location. The beam element has length L_e, cross-sectional area A and bending rigidity I.

2.1.1. Rectangular cross-sectional beam

The additional strain energy due to the existence of the crack can be expressed as [11,13]

$$\Pi_c = \int_{A_c} G \, \mathrm{d}A, \tag{1}$$

where G is the strain energy release rate function and A_c is the effective cracked area. The strain energy release rate function G can be expressed as [13]

$$G = \frac{1}{E'}[(K_{I1} + K_{I2} + K_{I3})^2 + K_{II2}^2], \tag{2}$$

where $E' = E$ for plane stress problem, $E' = E/(1-\mu^2)$ for plane strain problem; K_{I1}, K_{I2}, K_{I3} and K_{II2} are the stress intensity factors due to loads P_1, P_2 and P_3:

$$K_{I1} = \frac{P_1}{bh}\sqrt{\pi\xi}F_1\left(\frac{\xi}{h}\right), \quad K_{I2} = \frac{6P_2L_c}{bh^2}\sqrt{\pi\xi}F_2\left(\frac{\xi}{h}\right), \tag{3,4}$$

$$K_{I3} = \frac{6P_3}{bh^2}\sqrt{\pi\xi}F_2\left(\frac{\xi}{h}\right), \quad K_{II2} = \frac{P_2}{bh}\sqrt{\pi\xi}F_{II}\left(\frac{\xi}{h}\right), \tag{5,6}$$

$$F_1(s) = \sqrt{\frac{\mathrm{tg}(\pi s/2)}{(\pi s/2)}}\frac{0.752 + 2.02s + 0.37\,(1-\sin(\pi s/2))^3}{\cos(\pi s/2)} \quad (s = \xi/h), \tag{7}$$

$$F_2(s) = \sqrt{\frac{\mathrm{tg}(\pi s/2)}{(\pi s/2)}}\frac{0.923 + 0.199(1-\sin(\pi s/2))^4}{\cos(\pi s/2)} \quad (s = \xi/h), \tag{8}$$

$$F_{II}(s) = \frac{1.122 - 0.561s + 0.085s^2 + 0.180s^3}{\sqrt{1-s}} \quad (s = \xi/h), \tag{9}$$

in which ξ is the crack depth, F_1, F_2 and F_{II} are the correction factors for stress intensity factors. It is worth noting that a is the final crack depth while ξ is the crack depth during the process of penetrating from zero to the final depth.

Using Paris equation, we have

$$\delta_i = \frac{\partial \Pi_c}{\partial P_i} \quad (i = 1,2,3). \tag{10}$$

By definition, the elements of the overall additional flexibility matrix c_{ij} can be expressed as

$$c_{ij} = \frac{\partial \delta_i}{\partial P_j} = \frac{\partial^2 \Pi_c}{\partial P_i \partial P_j} \quad (i,\ j = 1,2,3). \tag{11}$$

Substituting Eqs. (3)–(6) into Eq. (2), then into Eqs. (1) and (11), and considering that all K's are independent of η, we obtain

$$c_{ij} = \frac{b}{E'}\frac{\partial^2}{\partial P_i \partial P_j}\int_0^a \left\{\left[\frac{P_1}{bh}\sqrt{\pi\xi}F_1\left(\frac{\xi}{h}\right) + \frac{6P_2L_c}{bh^2}\sqrt{\pi\xi}F_2\left(\frac{\xi}{h}\right) + \frac{6P_3}{bh^2}\sqrt{\pi\xi}F_2\left(\frac{\xi}{h}\right)\right]^2 + \frac{P_2^2}{b^2h^2}\pi\xi F_{II}^2\left(\frac{\xi}{h}\right)\right\} \mathrm{d}\xi \quad (i,\ j = 1,2,3). \tag{12}$$

From Eq. (12), the elements of the overall additional flexibility matrix c_{ij} can be obtained. All the elements c_{ij} are further expressed as dimensionless forms as follows (by setting $x = \xi/h$):

$$F(1,1) = c_{11}E'b = 2\pi \int_0^{a/h} xF_1^2(x)\,\mathrm{d}x, \tag{13}$$

$$F(1,2) = \frac{c_{12}E'bh}{L_c} = 12\pi \int_0^{a/h} xF_1(x)F_2(x)\,\mathrm{d}x, \tag{14}$$

$$F(1,3) = c_{13}E'bh = F(1,2), \tag{15}$$

$$F(2,2) = c_{22}E'b = 2\pi\left[\frac{36L_c^2}{h^2}\int_0^{a/h} xF_2^2(x)\,\mathrm{d}x + \int_0^{a/h} xF_{II}^2(x)\,\mathrm{d}x\right], \tag{16}$$

$$F(2,3) = \frac{c_{23}E'bh^2}{L_c} = 72\pi \int_0^{a/h} xF_2^2(x)\,\mathrm{d}x, \tag{17}$$

$$F(3,3) = c_{33}E'bh^2 = F(2,3). \tag{18}$$

Due to symmetry of the matrix C_{ovl} and F, only the upper triangular elements are listed in the above equations. The computations of Eqs. (13)–(18) are carried out by using 128-point Gauss quadrature [14]. The computed results are shown in Figs. 3 and 4. Fig. 3 shows the dimensionless flexibility coefficients $F(1,1)$, $F(1,2) = F(1,3)$, $F(2,3) = F(3,3)$ as a function of relative crack depth (a/h). It is worth noting that whilst the coefficients c_{12} and c_{23} are linearly dependent on the value of (L_c/h), $F(1,2)$ and $F(2,3)$ are independent of (L_c/h). It can be seen in Fig. 3 that the five flexibility coefficients increase as the crack depth a increases. Fig. 4 shows the dimensionless flexibility coefficient $F(2,2)$ as a function of relative crack depth a/h and for various distances L_c between the crack location and the beam end. $F(2, 2)$ is explicitly dependent on the value of (L_c/h). It can be seen from Fig. 4 that as L_c increases, the dimensionless flexibility coefficient

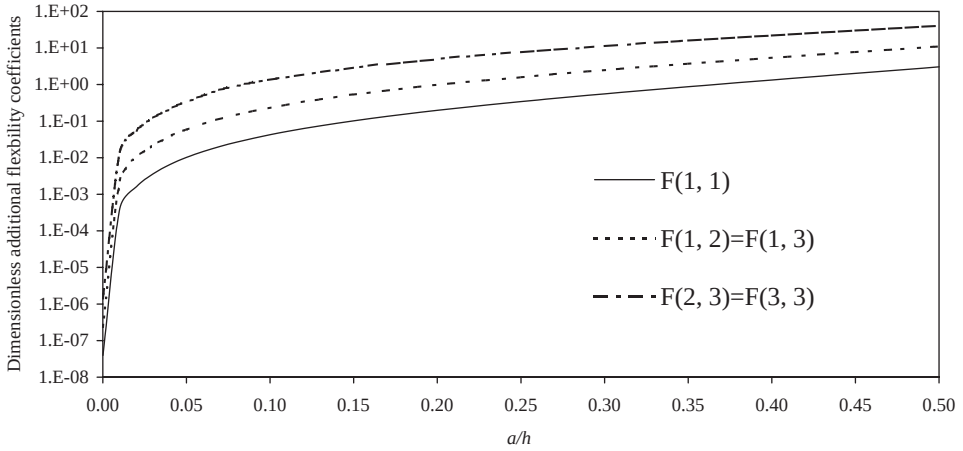

Fig. 3. Dimensionless additional flexibility coefficients of a rectangular cross-sectional beam.

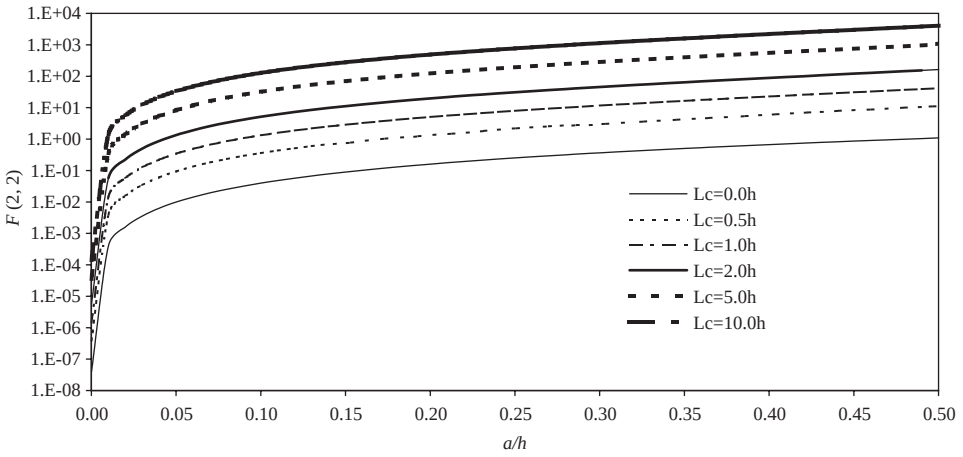

Fig. 4. Dimensionless additional flexibility coefficient $F(2,2)$ of a rectangular cross-sectional beam.

$F(2,2)$ increases significantly. In fact, from Eq. (16), one can see that the first part of $F(2,2)$ increases quadratically when the value of (L_c/h) increases. This is due to the increase in bending moment P_2L_c and hence the additional strain energy. In summary, the coefficients $c_{12}=c_{21}$, c_{22}, and $c_{23}=c_{32}$ are affected by the value of (L_c/h) while the coefficients c_{11}, $c_{13}=c_{31}$ and c_{33} are not affected by the value of (L_c/h); among all the elements of F matrix, only the element $F(2,2)$ is affected by the value of (L_c/h). The corresponding least squares best-fitted formulas are as follows:

$$\begin{aligned}F(1,1)\approx{}& e^{1/(1-x)}(-0.326584\times10^{-5}x+1.455190x^2-0.984690x^3+4.895396x^4\\&-6.501832x^5+12.792091x^6-26.723556x^7+35.073593x^8-34.954632x^9\\&+9.054062x^{10})\quad(0\leqslant x=a/h\leqslant0.5,\ error\leqslant0.009\%),\end{aligned}\tag{19}$$

$$\begin{aligned}F(1,2)\approx{}& e^{1/(1-x)}(-0.107478\times10^{-4}x+8.730431x^2-13.806738x^3+36.335828x^4\\&-64.758716x^5+102.695857x^6-171.543812x^7+211.600719x^8-192.273364x^9\\&+72.312335x^{10}\quad(0\leqslant x=a/h\leqslant0.5,\ error\leqslant0.005\%),\end{aligned}\tag{20}$$

$$\begin{aligned}F(2,2)={}& e^{1/(1-x)}(-0.326018\times10^{-6}x+1.454954x^2-1.455784x^3-0.421981x^4\\&-0.279522x^5+0.455399x^6-2.432830x^7+5.427219x^8-6.643057x^9\\&+4.466758x^{10})+(L_c/h)^2F(3,3)\quad(0\leqslant x=a/h\leqslant0.5,\ error\leqslant0.003\%),\end{aligned}\tag{21}$$

$$\begin{aligned}F(3,3)\approx{}& e^{1/(1-x)}(-0.219628\times10^{-4}x+52.379034x^2-130.248317x^3+308.442769x^4\\&-602.445544x^5+939.044538x^6-1310.950293x^7+1406.523682x^8-1067.499820x^9\\&+391.536356x^{10})\quad(0\leqslant x=a/h\leqslant0.5,\ error\leqslant0.002\%)\end{aligned}\tag{22}$$

In practice, we are interested in the early detection of cracks, and therefore the above best-fitted formulas are given with relative crack depth (a/h) limited in the scope of 0.5. Fig. 5 compares the

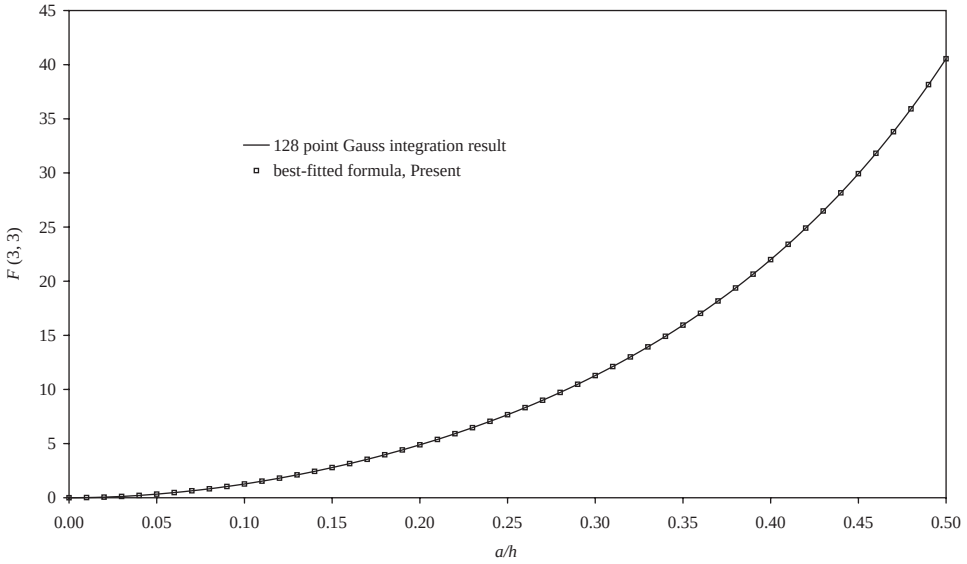

Fig. 5. Dimensionless additional flexibility coefficients of a rectangular cross-sectional beam.

results of 128-point Gauss integration with those obtained using the present best-fitted formula. From Fig. 5, it can be seen that the present best-fitted formula agrees perfectly with the Gauss integration result.

2.1.2. Circular cross-sectional beam

Fig. 2 shows a typical cracked beam element with circular cross-section. The geometrical dimensions are as follows:

$$\xi' = \xi + \sqrt{\frac{D^2}{4} - \eta^2} - \frac{D}{2}, \tag{23}$$

$$b(a) = \sqrt{Da - a^2}, \tag{24}$$

$$h'(\eta) = \sqrt{D^2 - 4\eta^2}, \tag{25}$$

$$a'(a,\eta) = \sqrt{\frac{D^2}{4} - \eta^2} - \left(\frac{D}{2} - a\right), \tag{26}$$

where D is the diameter of the beam. A similar procedure to the rectangular cross-sectional beam is used to derive the overall additional flexibility matrix for a circular cross-sectional beam. The additional strain energy due to the existence of the crack can be expressed as

$$\Pi_c = \int_{A_c} G\,\mathrm{d}A = \int_{-b(a)}^{b(a)} \left[\int_0^{a'(a,\eta)} G\,\mathrm{d}\xi' \right] \mathrm{d}\eta, \tag{27}$$

where G is the strain energy release rate function and A_c is the effective cracked area. The strain energy release rate function G can be related to the stress intensity factors as in Eq. (2), in which

$$K_{I1} = \frac{4P_1}{\pi D^2}\sqrt{\pi\xi'}F_1\left(\frac{\xi'}{h'}\right), \quad K_{I2} = \frac{32P_2L_ch'}{\pi D^4}\sqrt{\pi\xi'}F_2\left(\frac{\xi'}{h'}\right), \tag{28, 29}$$

$$K_{I3} = \frac{32P_3h'}{\pi D^4}\sqrt{\pi\xi'}\,F_2\left(\frac{\xi'}{h'}\right), \quad K_{II2} = \frac{4P_2}{\pi D^2}\sqrt{\pi\xi'}\,F_{II}\left(\frac{\xi'}{h'}\right), \tag{30, 31}$$

where ξ' is the crack penetrating depth of the strip. Substituting Eqs. (28)–(31) into Eq. (2), then into Eqs. (27) and (11) and considering Eqs. (23)–(26), the following expression can be derived:

$$c_{ij} = \frac{1}{E'}\frac{\partial^2}{\partial P_i\partial P_j}\int_{-\sqrt{Da-a^2}}^{\sqrt{Da-a^2}}\int_0^{\sqrt{(D^2/4-\eta^2)}-(D/2-a)}\left\{\left[\frac{4P_1}{\pi D^2}\sqrt{\pi\xi'}\,F_1\left(\frac{\xi'}{h'}\right)\right.\right.$$
$$\left.\left.+\frac{32P_2L_ch'}{\pi D^4}\sqrt{\pi\xi'}\,F_2\left(\frac{\xi'}{h'}\right)+\frac{32P_3h'}{\pi D^4}\sqrt{\pi\xi'}F_2\left(\frac{\xi'}{h'}\right)\right]^2+\frac{16P_2^2}{\pi D^4}\xi'F_{II}^2\left(\frac{\xi'}{h'}\right)\right\}\mathrm{d}\xi'\,\mathrm{d}\eta$$
$$(i,j=1,2,3). \tag{32}$$

From Eq. (32), the elements of the overall additional flexibility matrix c_{ij} can be obtained. All the elements c_{ij} are further expressed as dimensionless forms as follows (by setting $x=\xi/D$ and $y=\eta/D$):

$$F(1,1) = c_{11}E'D = \frac{32}{\pi}\int\int_{A_s}\left(x+\sqrt{\frac{1}{4}-y^2}-\frac{1}{2}\right)F_1^2\left(\frac{x+\sqrt{\frac{1}{4}-y^2}-\frac{1}{2}}{\sqrt{1-4y^2}}\right)\mathrm{d}x\,\mathrm{d}y, \tag{33}$$

$$F(1,2) = \frac{c_{12}E'D^2}{L_c} = \frac{256}{\pi}\int\int_{A_s}\sqrt{1-4y^2}\left(x+\sqrt{\frac{1}{4}-y^2}-\frac{1}{2}\right)$$
$$\times F_1\left(\frac{x+\sqrt{\frac{1}{4}-y^2}-\frac{1}{2}}{\sqrt{1-4y^2}}\right)\cdot F_2\left(\frac{x+\sqrt{\frac{1}{4}-y^2}-\frac{1}{2}}{\sqrt{1-4y^2}}\right)\mathrm{d}x\,\mathrm{d}y, \tag{34}$$

$$F(1,3) = c_{13}E'D^2 = F(1,2), \tag{35}$$

$$F(2,2) = c_{22}E'D = \frac{2048L_c^2}{\pi D^2}\int\int_{A_s}\sqrt{1-4y^2}\left(x+\sqrt{\frac{1}{4}-y^2}-\frac{1}{2}\right)$$
$$\times F_2^2\left(\frac{x+\sqrt{\frac{1}{4}-y^2}-\frac{1}{2}}{\sqrt{1-4y^2}}\right)\mathrm{d}x\,\mathrm{d}y+\frac{32}{\pi}\int\int_{A_s}\left(x+\sqrt{\frac{1}{4}-y^2}-\frac{1}{2}\right)$$
$$\times F_{II}^2\left(\frac{x+\sqrt{\frac{1}{4}-y^2}-\frac{1}{2}}{\sqrt{1-4y^2}}\right)\mathrm{d}x\,\mathrm{d}y, \tag{36}$$

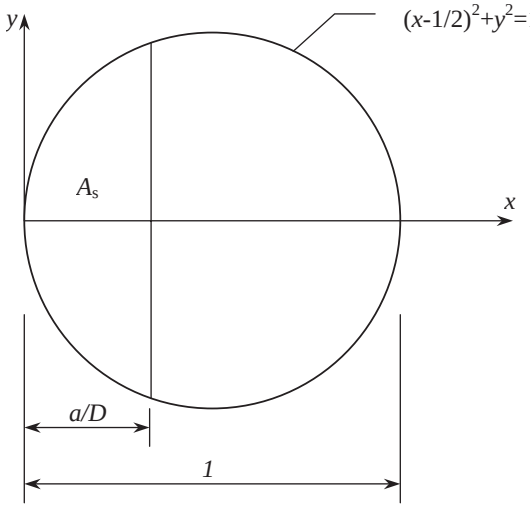

Fig. 6. Integration area A_s for calculating the additional flexibility matrix of a beam with circular cross-section.

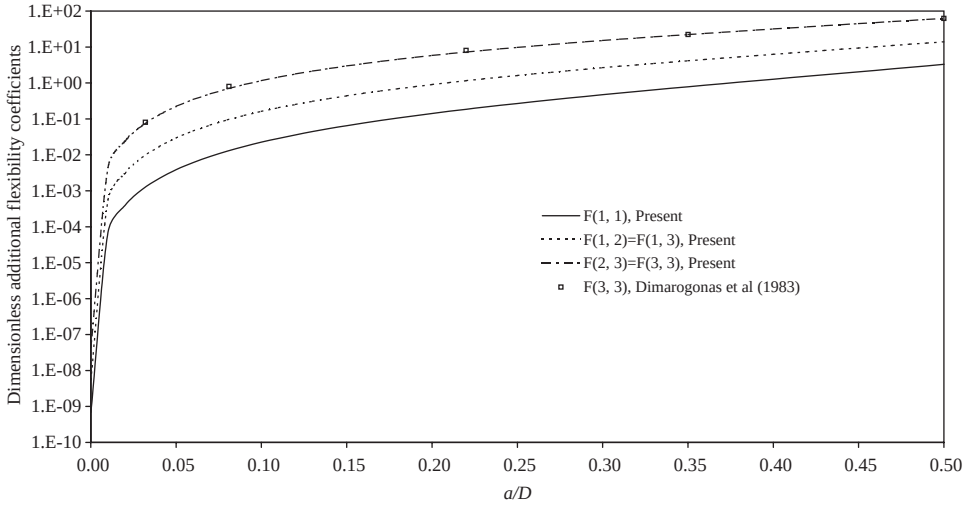

Fig. 7. Dimensionless additional flexibility coefficients of a circular cross-sectional beam.

$$F(2,3)=\frac{c_{23}E'D^3}{L_c}=\frac{2048}{\pi}\int\int_{A_s}\sqrt{1-4y^2}\left(x+\sqrt{\frac{1}{4}-y^2}-\frac{1}{2}\right)\times F_2^2\left(\frac{x+\sqrt{\frac{1}{4}-y^2}-\frac{1}{2}}{\sqrt{1-4y^2}}\right)\mathrm{d}x\,\mathrm{d}y, \tag{37}$$

$$F(3,3)=c_{33}E'D^3=F(2,3), \tag{38}$$

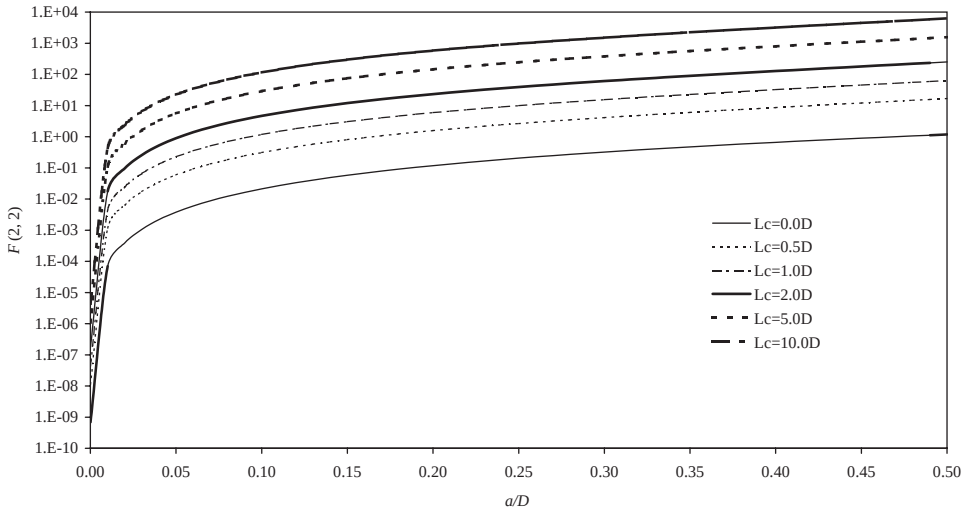

Fig. 8. Dimensionless additional flexibility coefficient $F(2,2)$ of a circular cross-sectional beam.

where A_s is the integration area in a unit circle as shown in Fig. 6. The computations of Eqs. (33)–(38) are carried out by using 128×128 Gauss quadrature [14]. The computed results are shown in Figs. 7 and 8. Fig. 7 shows the coefficients of the overall additional flexibility matrix elements $F(1,1)$, $F(1,2) = F(1,3)$, $F(2,3) = F(3,3)$ as a function of the relative crack depth (a/D). Fig. 8 shows the dimensionless flexibility coefficient $F(2,2)$ as a function of relative crack depth (a/D) and for various distances L_c between the crack location and the beam end. It can be seen from Fig. 7 that the present integration result $F(3,3)$ agrees very well with that of Dimarogonas et al. [11]. The corresponding least-squares best-fitted formulas are as follows:

$$\begin{aligned} F(1,1) \approx\ & e^{1(1-x)}(-0.123234x^{0.4} + 3.156480x^{0.8} - 34.490509x^{1.2} + 211.429280x^{1.6} \\ & - 802.944428x^{2} + 1964.215885x^{2.4} - 3092.084441x^{2.8} + 3036.531592x^{3.2} \\ & - 1692.594137x^{3.6} + 411.505609x^{4}) \quad (0 \leqslant x = a/D \leqslant 0.5,\ error \leqslant 1.96\%), \end{aligned} \tag{39}$$

$$\begin{aligned} F(1,2) \approx\ & e^{1/(1-x)}(0.0525646x^{0.4} - 1.694740x^{0.8} + 22.910177x^{1.2} - 171.535649x^{1.6} \\ & + 789.046673x^{2} - 2318.500920x^{2.4} + 4461.869140x^{2.8} - 5337.583060x^{3.2} \\ & + 3599.915932x^{3.6} - 1044.227437x^{4}) \quad (0 \leqslant x = a/D \leqslant 0.5,\ error \leqslant 1.3\%), \end{aligned} \tag{40}$$

$$\begin{aligned} F(2,2) \approx\ & e^{1/(1-x)}(-0.0181106x^{0.4} + 0.483199x^{0.8} - 5.519102x^{1.2} + 35.485789x^{1.6} \\ & - 141.871055x^{2} + 367.853395x^{2.4} - 610.901666x^{2.8} + 639.711620x^{3.2} \\ & - 384.398763x^{3.6} + 98.728659x^{4}) + (L_c/D)^2 F(3,3) \\ & (0 \leqslant x = a/D \leqslant 0.5,\ error \leqslant 1.2\%), \end{aligned} \tag{41}$$

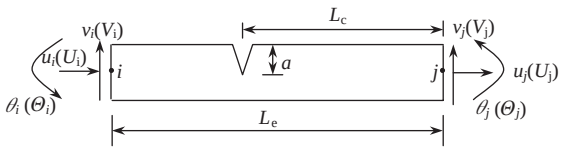

Fig. 9. A typical cracked beam element subjected to axial force, shearing force and bending moment (under the conventional FEM co-ordinate system).

$$F(3,3) \approx e^{1/(1-x)}(0.102895x^{0.4} - 3.653566x^{0.8} + 53.161890x^{1.2} - 423.977411x^{1.6} + 2072.129084x^{2} - 6447.218742x^{2.4} + 13613.390334x^{2.8} - 17873.887075x^{3.2} + 12985.643127x^{3.6} - 3999.171110x^{4}) \quad (0 \leqslant x = a/D \leqslant 0.5,\ error \leqslant 0.49\%). \tag{42}$$

2.2. Overall additional flexibility matrix C_{ovl} under the conventional FEM co-ordinate system

Fig. 9 shows a typical cracked beam element under the conventional FEM co-ordinate and notation system. Under the FEM co-ordinate and notation system, the relationship between the displacement and the forces can be expressed as

$$\begin{Bmatrix} u_j - u_i \\ v_j - v_i - L_e\theta_i \\ \theta_j - \theta_i \end{Bmatrix} = C_{ovl} \begin{Bmatrix} U_j \\ V_j \\ \Theta_j \end{Bmatrix}, \quad \text{where } C_{ovl} = \begin{bmatrix} c_{11} & -c_{12} & -c_{13} \\ -c_{21} & c_{22} & c_{23} \\ -c_{31} & c_{32} & c_{33} \end{bmatrix}. \tag{43,44}$$

It is worth noting that the local flexibility matrix C_{loc} can be obtained from the overall flexibility matrix C_{ovl} by setting $L_c = 0$:

$$C_{loc} = C_{ovl}|_{L_c=0}. \tag{45}$$

2.3. Flexibility matrix C_{intact} of the intact beam element

The flexibility matrix C_{intact} of the intact beam element can be written as

$$\begin{Bmatrix} u_j - u_i \\ v_j - v_i - L_e\theta_i \\ \theta_j - \theta_i \end{Bmatrix} = C_{intact} \begin{Bmatrix} U_j \\ V_j \\ \Theta_j \end{Bmatrix}, \quad \text{where } C_{intact} = \begin{bmatrix} \dfrac{L_e}{EA} & 0 & 0 \\ 0 & \dfrac{L_e^3}{3EI} & \dfrac{L_e^2}{2EI} \\ 0 & \dfrac{L_e^2}{2EI} & \dfrac{L_e}{EI} \end{bmatrix}. \tag{46,47}$$

2.4. Total flexibility matrix C_{tot} of the cracked beam element

The total flexibility matrix C_{tot} of the cracked beam element can now be obtained by

$$C_{tot} = C_{intact} + C_{ovl} = \begin{bmatrix} \frac{L_e}{EA} + c_{11} & -c_{12} & -c_{13} \\ -c_{21} & \frac{L_e^3}{3EI} + c_{22} & \frac{L_e^2}{2EI} + c_{23} \\ -c_{31} & \frac{L_e^2}{2EI} + c_{32} & \frac{L_e}{EI} + c_{33} \end{bmatrix}. \tag{48}$$

2.5. Stiffness matrix K_c of a cracked beam element

Through the equilibrium conditions, the stiffness matrix K_c of a cracked beam element can be obtained as follows [9,10]:

$$K_c = LC_{tot}^{-1}L^{\mathrm{T}} \tag{49}$$

where

$$L = \begin{bmatrix} -1 & 0 & 0 \\ 0 & -1 & 0 \\ 0 & -L_e & -1 \\ 1 & 0 & 0 \\ 0 & 1 & 0 \\ 0 & 0 & 1 \end{bmatrix}. \tag{50}$$

3. Interpolation shape function for a cracked beam element

For computing the correct vibration modes of a cracked beam, it is necessary to construct the interpolation shape function that can satisfy the local flexibility conditions at the crack locations. Fig. 10 shows a typical cracked beam element and the associated degrees of freedom.

The interpolation shape functions $u(x)$ and $v(x)$ can be expressed as:

$$u_-(x) = L_1(x, x_c)u_i + L_2(x, x_c)u_c^-, \quad 0 \leqslant x \leqslant x_c, \tag{51}$$

$$u_+(x) = L_1(x - x_c, L_c)u_c^+ + L_2(x - x_c, L_c)u_j, \quad x_c \leqslant x \leqslant L_e, \tag{52}$$

$$v_-(x) = H_1(x, x_c)v_i + H_2(x, x_c)\theta_i + H_3(x, x_c)v_c^- + H_4(x, x_c)\theta_c^-, \quad 0 \leqslant x \leqslant x_c, \tag{53}$$

$$\begin{aligned} v_+(x) = {} & H_1(x - x_c, L_c)v_c^+ + H_2(x - x_c, L_c)\theta_c^+ + H_3(x - x_c, L_c)v_j \\ & + H_4(x - x_c, L_c)\theta_j, \quad x_c \leqslant x \leqslant L_e, \end{aligned} \tag{54}$$

where $u_-(x)$ and $v_-(x)$ denote the deformation of the beam from the left hand side end node i to the location of the crack, while $u_+(x)$ and $v_+(x)$ denote the deformation of beam from the location

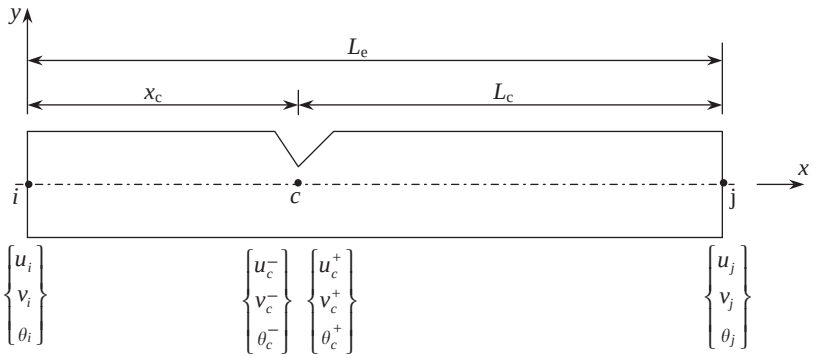

Fig. 10. Interpolation shape function for a cracked beam element.

of the crack to the right hand side end node j. The L's and H's are Lagrangian and Hermitian interpolation base function, respectively, and are given by:

$$L_1(x,L) = 1 - \frac{x}{L}, \quad L_2(x,L) = \frac{x}{L}, \tag{55, 56}$$

$$H_1(x,L) = \left(1 - \frac{x}{L}\right)^2 \left(\frac{2x}{L} + 1\right), \quad H_2(x,L) = \left(1 - \frac{x}{L}\right)^2 x, \tag{57, 58}$$

$$H_3(x,L) = \left(\frac{x}{L}\right)^2 \left(-\frac{2x}{L} + 3\right), \quad H_4(x,L) = \left(\frac{x}{L}\right)^2 (x - L). \tag{59, 60}$$

The local flexibility conditions at the location of the crack can be expressed as

$$\begin{Bmatrix} u_c^+ - u_c^- \\ v_c^+ - v_c^- \\ \theta_c^+ - \theta_c^- \end{Bmatrix} = C_{loc} \begin{Bmatrix} U_c^+ \\ V_c^+ \\ \Theta_c^+ \end{Bmatrix} = C_{loc} \begin{bmatrix} EA & 0 & 0 \\ 0 & -EI & 0 \\ 0 & 0 & EI \end{bmatrix} \begin{Bmatrix} u'_+(x_c) \\ v'''_+(x_c) \\ v''_+(x_c) \end{Bmatrix}. \tag{61}$$

The continuity conditions at the crack location can be expressed as

$$u'_-(x_c) = u'_+(x_c), \quad v''_-(x_c) = v''_+(x_c), \quad v'''_-(x_c) = v'''_+(x_c). \tag{62–64}$$

By grouping Eqs. (61)–(64), we can obtain

$$\delta_c = A^{-1} B \delta, \tag{65}$$

where

$$\delta_c = [u_c^- \;\; v_c^- \;\; \theta_c^- \;\; u_c^+ \;\; v_c^+ \;\; \theta_c^+]^{\mathrm{T}}, \tag{66}$$

$$\delta = [u_i \;\; v_i \;\; \theta_i \;\; u_j \;\; v_j \;\; \theta_j]^{\mathrm{T}}, \tag{67}$$

$$A = \begin{bmatrix} -1 & 0 & 0 & 1+\frac{EAc_{11}}{L_c} & -\frac{6EIc_{13}}{L_c^2} & -\frac{4EIc_{13}}{L_c} \\ 0 & -1 & 0 & 0 & 1+\frac{12EIc_{22}}{L_c^3} & \frac{6EIc_{22}}{L_c^2} \\ 0 & 0 & -1 & -\frac{EAc_{31}}{L_c} & \frac{6EIc_{33}}{L_c^2} & 1+\frac{4EIc_{33}}{L_c} \\ \frac{1}{x_c} & 0 & 0 & \frac{1}{L_c} & 0 & 0 \\ 0 & -\frac{6}{x_c^2} & \frac{4}{x_c} & 0 & \frac{6}{L_c^2} & \frac{4}{L_c} \\ 0 & -\frac{12}{x_c^3} & \frac{6}{x_c^2} & 0 & -\frac{12}{L_c^3} & -\frac{6}{L_c^2} \end{bmatrix}, \tag{68}$$

$$B = \begin{bmatrix} 0 & 0 & 0 & \frac{EAc_{11}}{L_c} & -\frac{6EIc_{13}}{L_c^2} & \frac{2EIc_{13}}{L_e} \\ 0 & 0 & 0 & 0 & \frac{12EIc_{22}}{L_c^3} & -\frac{6EIc_{22}}{L_c^2} \\ 0 & 0 & 0 & -\frac{EAc_{31}}{L_c} & \frac{6EIc_{33}}{L_c^2} & -\frac{2EIc_{33}}{L_c} \\ \frac{1}{x_c} & 0 & 0 & \frac{1}{L_c} & 0 & 0 \\ 0 & -\frac{6}{x_c^2} & -\frac{2}{x_c} & 0 & \frac{6}{L_c^2} & -\frac{2}{L_c} \\ 0 & -\frac{12}{x_c^3} & -\frac{6}{x_c^2} & 0 & -\frac{12}{L_c^3} & \frac{6}{L_c^2} \end{bmatrix}. \tag{69}$$

It is important to note that the deformation of the beam at the crack location is successfully related to the deformation of the beam at the two end nodes of the beam element through Eq. (65). It should be pointed out that all the c_{ij}'s in Eqs. (68) and (69) are elements of the local flexibility matrix C_{loc}.

4. Numerical examples

Example 1. (*A cantilevered beam with a crack located at the clamped end*). Shifrin et al. [2] obtained the frequency reductions of a cracked cantilever beam with a crack at the clamped end, as shown in Fig. 11, by building up and solving the differential vibration equations piecewisely. Their results can be viewed as accurate except for the error in the root searching process. In this paper, the finite element results are compared with those obtained by Shifrin et al. in order to validate the proposed theory. The geometrical properties of the beam are length $L = 0.8$ m, and rectangular cross-section of width $b = 0.02$ m and height $h = 0.02$ m. The physical properties of

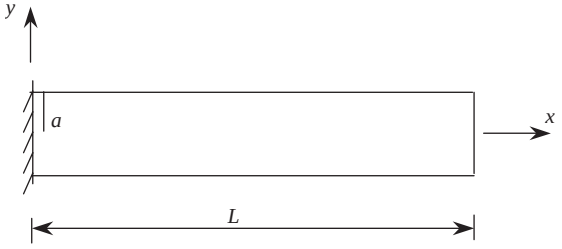

Fig. 11. A cantilevered beam with a crack at the clamped end.

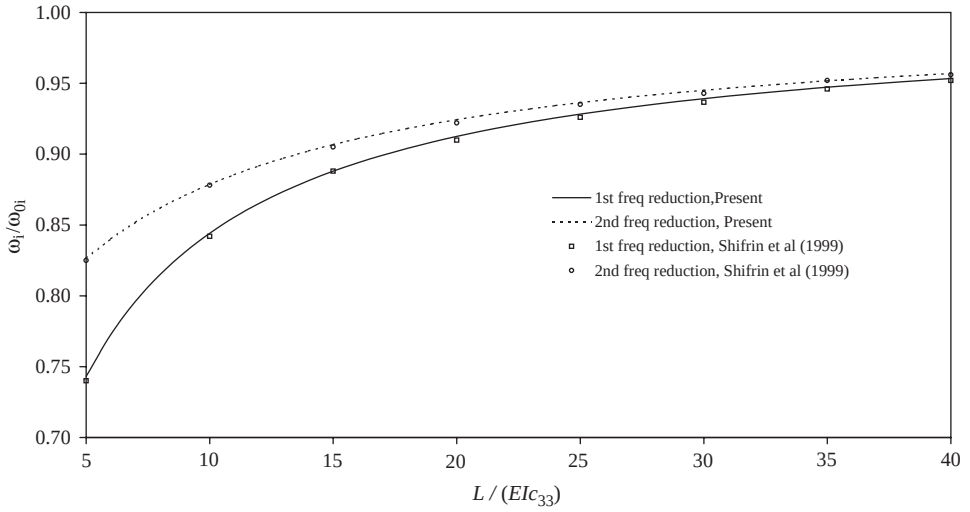

Fig. 12. Frequency reduction of a cantilever beam having a single crack at the clamped end.

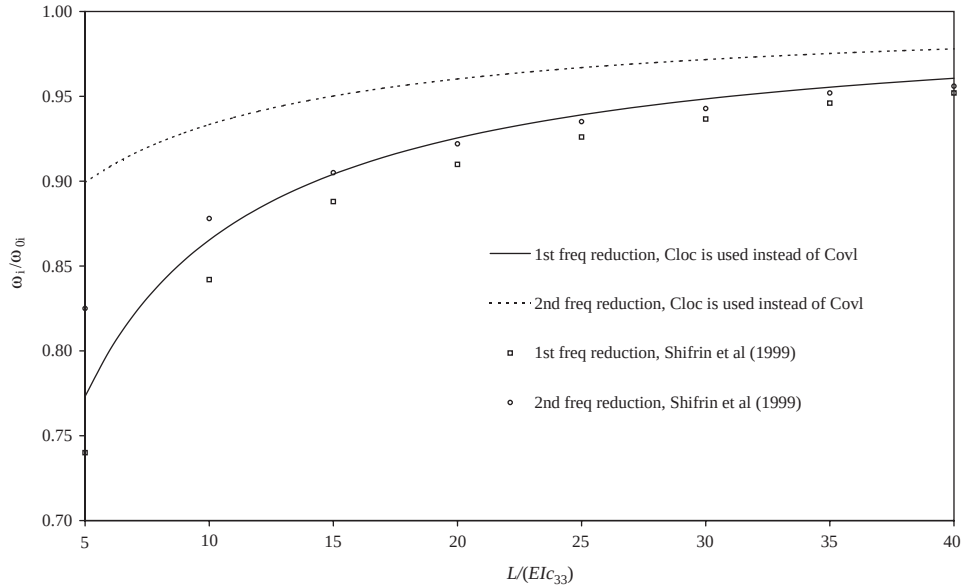

Fig. 13. Frequency reduction of a cantilever beam having a single crack at the clamped end.

the beam are Young's modulus $E = 206$ GPa, the Poisson ratio $\mu = 0.3$, and density $\rho = 7800\ \mathrm{kg/m^3}$. The beam is divided into 16 equal elements. In Fig. 12, the results obtained by the present method are compared with the results from Ref. [2], where ω_i is the natural frequency of the cracked beam, ω_{0i} is the natural frequency of the corresponding uncracked beam, and ω_i/ω_{0i} is the frequency reduction. Very good agreement between the two methods can be observed. Fig. 13 shows the results obtained when the local flexibility matrix C_{loc} instead of the overall

additional flexibility matrix C_{ovl} is used in the formation process of the total flexibility matrix (see Eq. (48)). It can be seen that the discrepancies between the FEM and the analytical method are significant if C_{loc} is used instead of C_{ovl}.

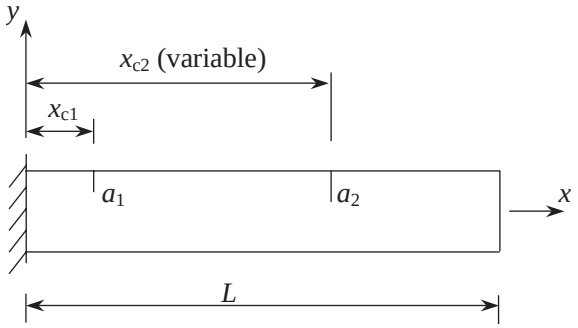

Fig. 14. A cantilevered beam with two cracks while the location of the second crack is variable.

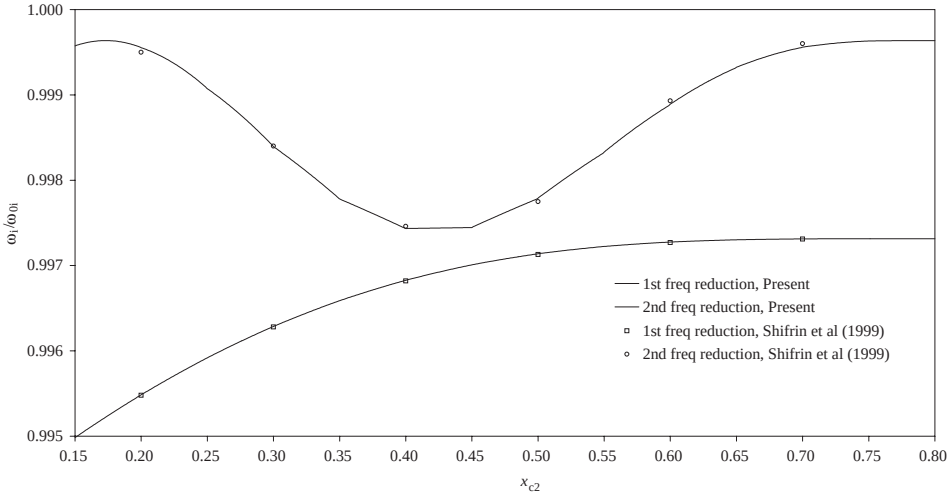

Fig. 15. Effect of the second crack location on the natural frequencies of the beam ($x_{c1} = 0.12$ m, $a_1 = 0.002$ m, x_{c2} is variable, $a_2 = 0.002$ m).

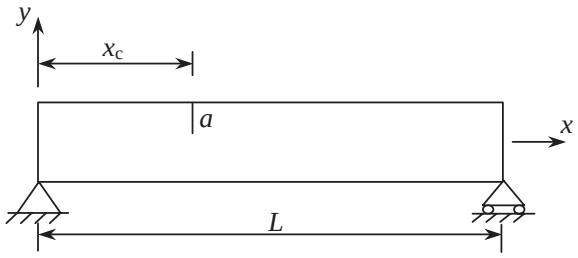

Fig. 16. A simply supported shaft with a crack.

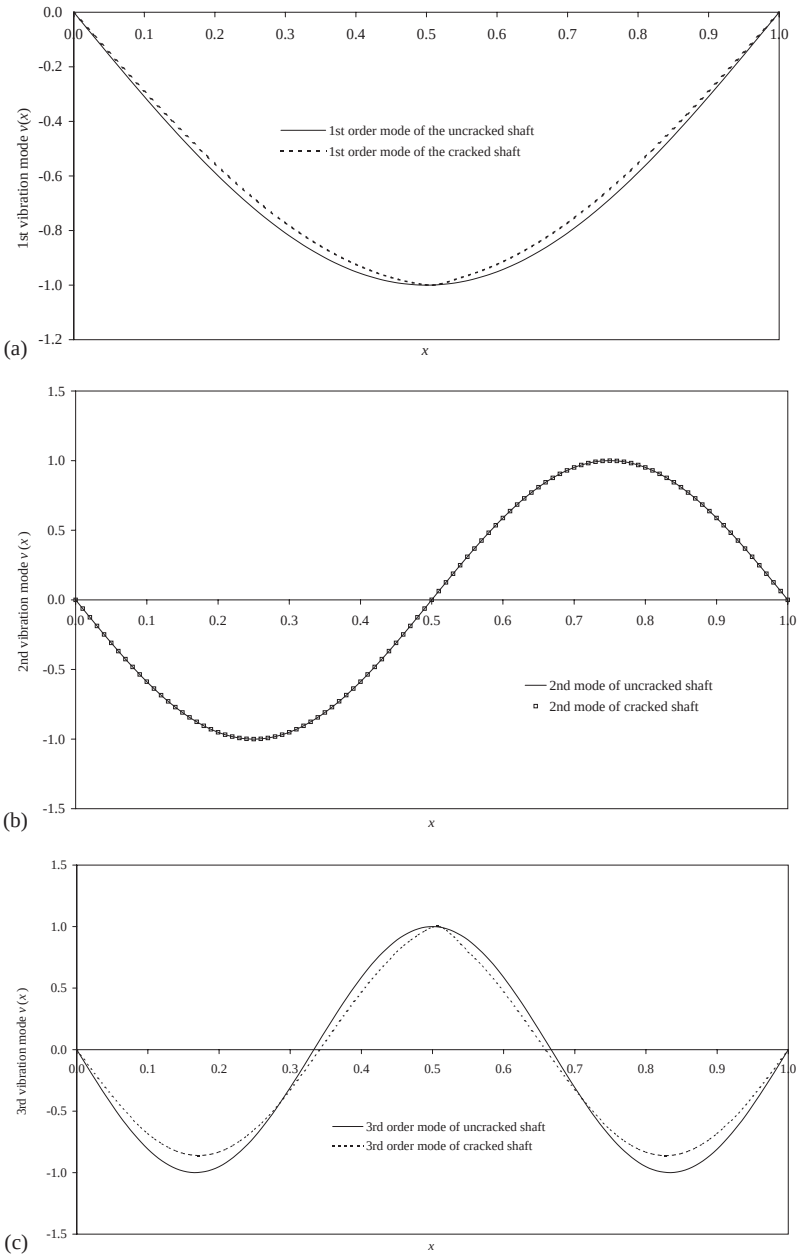

Fig. 17. (a) First vibration mode of a simply supported shaft with a crack located at $x_c = 0.5$ m ($f_1 = 55.92$ Hz, $f_1/f_{01} = 0.9237$). (b) Second vibration mode of a simply supported shaft with a crack located at $x_c = 0.5$ m ($f_2 = 242.18$ Hz, $f_2/f_{02} = 0.9999$). (c) Third vibration mode of a simply supported shaft with a crack located at $x_c = 0.5$ m ($f_3 = 506.85$ Hz, $f_3/f_{03} = 0.9301$).

Example 2. (*A cantilevered beam with two cracks*). Fig. 14 shows a cantilevered beam with two cracks. The beam has the same geometrical and physical parameters as those given in Example 1. The first crack is at a fixed location of $x_{c1} = 0.12$ m and has a depth $a_1 = 2$ mm. The location of

the second crack varies from the left end to the right end of the beam, with a fixed depth of $a_2 = 2$ mm. Both the results obtained by the present method and those from Ref. [2] are shown in Fig. 15. Good agreements are again observed.

Example 3. (*Vibration mode of a cracked simply supported shaft*). Fig. 16 shows a simply supported beam with a crack. The geometrical and physical properties of the shaft are length $L = 1.0$ m, diameter $D = 0.03$ m, Young's modulus $E = 206$ GPa, density $\rho = 7800$ kg/m^3 and the Poisson ratio $\mu = 0.3$. The crack is assumed to be at the centre of the beam and has a depth 0.015 m. The shaft was divided into 20 elements. Figs. 17(a)–(c) show the first three vibration modes of the cracked simply supported shaft for the natural frequencies of $f_1 = 55.92$ Hz ($f_1/f_{01} = 0.9237$), $f_2 = 242.18$ Hz ($f_2/f_{02} = 0.9999$) and $f_3 = 506.85$ Hz ($f_3/f_{03} = 0.9301$), respectively. It can be seen from Figs. 17(a) and (c) that the first and third order vibration modes are significantly different from those of un-cracked shaft, while the second order vibration mode (Fig. 17(b)) has almost no change. This is because the crack location is at the point where the second mode bending moment is zero, that is, $M_2(x)_{x=L/2} = 0$. These results demonstrate again that the bending moment and opening type of the crack dominate the behaviour of a cracked beam.

5. Conclusions

In this paper, the overall additional flexibility matrix instead of the local additional flexibility matrix is used to obtain the total flexibility matrix of a cracked beam. The stiffness matrix is then obtained from the total flexibility matrix. As a result, more accurate natural frequencies of a cracked beam are obtained. All the elements of the overall additional flexibility matrix have been computed by using 128-point (1D) or 128×128-point (2D) Gauss quadrature, and then best fitted using the least-squares method. A new shape interpolation function has been successfully developed to compute the vibrational modes of a cracked beam, which can perfectly satisfy the local flexibility conditions at the crack locations.

References

[1] C.A. Papadopoulos, A.D. Dimarogonas, Coupled longitudinal and bending vibrations of a rotating shaft with an open crack, *Journal of Sound and Vibration* 117 (1) (1987) 81–93.
[2] E.I. Shifrin, R. Ruotolo, Natural frequencies of a beam with an arbitrary number of cracks, *Journal of Sound and Vibration* 222 (1999) 409–423.
[3] D.Y. Zheng, S.C. Fan, Natural frequencies of a non-uniform beam with multiple cracks via modified Fourier series, *Journal of Sound and Vibration* 242 (4) (2001) 701–717.
[4] D.Y. Zheng, S.C. Fan, Natural frequency changes of a cracked Timoshenko beam by modified Fourier series, *Journal of Sound and Vibration* 246 (2) (2001) 297–317.
[5] S.C. Fan, D.Y. Zheng, F.T.K. Au, Gibbs phenomenon free Fourier series for vibration and stability of complex beams, *American Institute of Aeronautics and Astronautics Journal* 39 (10) (2001) 1977–1984.
[6] Y. Bamnios, E. Douka, A. Trochidis, Crack identification in beam structures using mechanical impedance, *Journal of Sound and Vibration* 256 (2) (2002) 287–297.
[7] J. Fernandez-Saez, L. Rubio, C. Navarro, Approximate calculation of the fundamental frequency for bending vibrations of cracked beams, *Journal of Sound and Vibration* 225 (2) (1999) 345–352.

[8] N.T. Khiem, T.V. Lien, A simplified method for natural frequency analysis of a multiple cracked beam, *Journal of Sound and Vibration* 245 (4) (2001) 737–751.
[9] A.S. Sekhar, B.S. Prabhu, Crack detection and vibration characteristics of cracked shafts, *Journal of Sound and Vibration* 157 (2) (1992) 375–381.
[10] A.S. Sekhar, Vibration characteristics of a cracked rotor with two open cracks, *Journal of Sound and Vibration* 223 (4) (1999) 497–512.
[11] A.D. Dimarogonas, C.A. Papadopoulos, Vibration of cracked shafts in bending, *Journal of Sound and Vibration* 91 (4) (1983) 583–593.
[12] R.F. Rizos, N. Aspragathos, A.D. Dimarogonas, Identification of crack location and magnitude in a cantilever beam from the vibration modes, *Journal of Sound and Vibration* 138 (3) (1990) 381–388.
[13] H. Tada, P.C. Paris, G.R. Irwin, *The Stress Analysis of Cracks Handbook*, ASME Press, New York, 2000.
[14] P.J. Davis, P. Rabinowitz, *Methods of Numerical Integration*, Academic Press, New York, 1975.